

ELECTROCHEMICAL NOISE SIGNAL PROCESSING USING R/S ANALYSIS AND FRACTIONAL FOURIER TRANSFORM

Rongtao Sun¹, Nikita Zaveri², YangQuan Chen¹, Anhong Zhou², Nephi Zufelt³

¹*Center for Self-Organizing and Intelligent Systems (CSOIS),
Department of Electrical Computer Engineering, Utah State University,
4120 Old Main Hill, Logan, Utah 84322-4120, Email: yqchen@ece.usu.edu*

²*Department of Biological and Irrigation Engineering, Utah State University,
4105 Old Main Hill, Logan, Utah 84322-4105. Email: azhou@cc.usu.edu*

³*Department of Mechanical and Aerospace Engineering, Utah State University,
4130 Old Main Hill, Logan, Utah 84322-4130.*

Abstract: The corrosion processes of stainless steel under different solutions were examined using Electrochemical Noise (ECN). Using Rescaled Range analysis, we demonstrated that ECN signals produced by corrosion processes have non-stationary and self-similar properties. The comparison and analysis of ECN signals in both time and frequency domain showed that the conventional methods failed to give out the differences of the ECN signals obtained under different solutions. Therefore, we introduced fractional Fourier transform (FrFT) to process ECN signals, which is a powerful tool for the time-frequency analysis of self similar signals that can better describe the corrosion behaviours of the electrode in different solutions.

Keywords: Electrochemical noise, Stainless steel, Self-similar signals, Rescaled range analysis, Fractional Fourier transform, Spectral noise impedance.

1. INTRODUCTION

One of the most important properties of any biomaterial which is used as a bioimplant is safety. Metals and alloys are widely used as biomedical materials in medical and dental devices, and the biocompatibility of a metallic alloy is closely associated with the interaction of the alloy with the surrounding environment. Metal release from the implant into the surrounding tissue may occur as a consequence of various mechanisms like (1) mechanical nature i.e. due to wear phenomena. (2) electrochemical nature i.e. corrosion processes. The implantation of a metal object into the body inevitably leads to some degree of local tissue response depending on the material utilized, possibly also induces a reaction in cells distant from the site of surgery. These reactions may be merely moderate or transient, but in more severe cases, serious tissue damage with permanent morphological and structural changes can occur.

Corrosion is defined as a chemical or an electrochemical reaction between a material usually a metal, and its environment that produces a deterioration of the metal and its properties.

Stainless Steel (SS) was first identified as a suitable material for orthopaedic implants. Till today, it is still one of the most frequently used biomaterial for implants because of its suitable mechanical properties and excellent clinical track record. Also, Stainless Steel (SS) has very low corrosion resistance and has low production costs (Meredith, *et al.*, 2005). Electrochemical noise (ECN) (Lowe and Eren, 2000; Lowe, 2002) is a technique whereby biocorrosion information is extracted from fluctuations either in potential or current that is observed on a corroding electrode. In this study, the corrosion behaviors of the stainless steel (SS) electrode in three artificial saliva solutions (Duffó and Castillo, 2004) were studied by using the Zero Resistance Ammeter (ZRA). In the ZRA measurement configuration, two identical electrodes (materials and size), namely,

working electrodes (WE) and counter electrode (CE), are immersed in the solution of interest. The fluctuation of the potential of WE and CE versus reference electrode (RE) as well as the coupling current between WE and CE will be measured simultaneously. ZRA is simply a current to voltage converter. It gives a voltage output proportional to the current flowing between its two input terminals while imposing a 'zero' voltage drop to the external circuit. The ZRA is an application for the measurement of the galvanic coupling current of dissimilar metals. Here, the coupling current is measured between two Stainless Steel electrodes.

Figure 1 shows an example of electrochemical noise responses obtained from a stainless steel electrode which was exposed to the artificial saliva solution for 5 min. This ECN data typically consists of three sets of measurements, the corrosion potential of the working electrode (WE), the counter electrode (CE), and the coupling current between WE and CE. In this study, we use the potential of WE for signal processing.

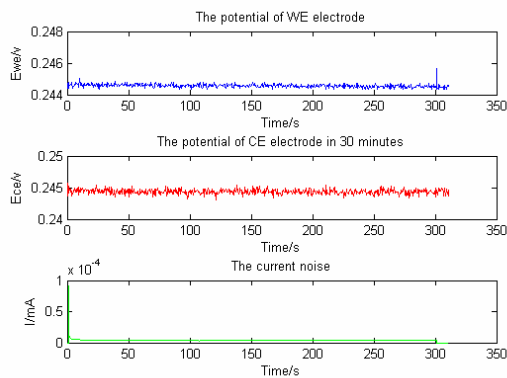


Figure 1: An example of ECN measurement. Top: potential noise of the WE electrode; middle: potential noise of the CE electrode; bottom: the corresponding coupling current between WE and CE. Solution used: Tomasi's artificial saliva solution; Electrode material: stainless steel.

A stochastic model of the similar ECN signal as above, obtained from the electrolysis current during bubble evolution, was reported by Gabrielli, *et al.* (1985). The experimental power spectral density (PSD) was in agreement with the theoretical model. Therefore, the PSD of the fluctuations generated by a stainless steel electrode at the corrosion potential can be used for measuring the corrosion rate.

The empirical ECN analysis methods, statistical or Fourier spectral methods (Gabrielli, *et al.*, 1985), were developed under the assumption that stochastic model is Gaussian distributed. However, these signals generally have significant impulsion in the waves of time domain, and their autocorrelation may have thick tails which are self-similar properties. This paper presents rescaled range (R/S) analysis (Leontitsis, 2004) to show the self similar property of ECN signals of stainless steel. Hurst (1965) developed the rescaled range analysis, a statistical method to analyze long records of natural phenomena.

Recently, fractional Fourier transform was found to be a powerful tool for the time-frequency analysis of self-similar signals. It has been successfully used

for many applications, such as optical systems and optical signal processing (Ozaktas, *et al.*, 1994), swept-frequency filters (Almeida, 1994), time-variant filtering and multiplexing (Ozaktas, *et al.*, 1994), pattern recognition (Mendlovic, *et al.*, 1995), and study of time-frequency distributions (Fonollosa and Nikias, 1994). The algorithm of Fractional Fourier transform used in this paper is obtained from Ozaktas, *et al.* (1996). For signals with time-bandwidth product N , the presented algorithm computes the fractional transform in $O(N \log N)$ time.

2. EXPERIMENTAL APPROACH

2.1 Materials Used

(1) EXPERIMENTAL SETUP:

Stainless Steel electrode was used as both working and counter electrode. The electrodes were prepared by polishing it with the polishing pads. Polishing pads were used to clean the stainless steel surface before the start of every new experiment. The electrodes were then thoroughly rinsed off with distilled water and they were made ready to use. Ag/AgCl reference electrode (CH Instruments, TX) was used. All the measurements were performed in room temperature.

VMP2/Z (PAR, TN) is used for ECN measurement. Zero Resistance Ammeter (ZRA) is a built-in technique in the multichannel potentiostat. Details about the software and the parameters for the ECN measurement are as follows:

Software: EC-Lab for Windows v9.01
 CE vs. WE compliance from -10 V to 10 V
 Electrode connection: standard
 Electrode surface area: 0.001 cm²
 tR1 (h:m:s): 0:00:10.0000
 dtR1 (s): 0.5000
 ti (h:m:s): 0:30:0.0000
 I Range: Auto
 Bandwidth: 5

The ECN measurement was conducted in each of these solutions for 30 min.

(2) TEST SOLUTIONS

The following different types of simulated saliva solutions were used for the ECN measurement. The constituents of individual solution were listed in Tables 1-3.

Solution A - Jenkin's Solution

Table 1: Chemical composition of the Jenkin's artificial saliva solution

Constituents	g/250mL
NaCl	0.2125
KCl	0.3000
CaCl ₂ ·2H ₂ O	0.0375
MgCl ₂ ·6H ₂ O	0.0125
K ₂ HPO ₄	0.0875
KSCN	0.0250
NaF	0.0025
H ₂ O ₂	0.0750
Sorbic Acid	0.0125

Solution B - Tomasi's Solution

Table 2: Chemical composition of the Tomasi's artificial saliva solution

Constituents	g/250mL
NaCl	0.1685
KCl	0.2400
CaCl ₂ .2H ₂ O	0.02925
MgCl ₂ .6H ₂ O	0.010125
K ₂ HPO ₄	0.02275

Solution C – NaCl Solution

Table 3: Chemical composition of the NaCl artificial saliva solution

Constituents	g/250mL
NaCl	2.5

3. RESCALED RANGE ANALYSIS

Self-similar random processes were introduced by Mandelbrot, *et al.* (1968) to model the long run behavior. A rescaled range (R/S) statistics method was proposed (Feder, 1988) to evaluate the Hurst exponent (H) in order to determine self-similar properties. It was shown that $0.5 < H < 1$ indicates the presence of self-similar properties and when $0 < H < 0.5$, there is antipersistence (Devynck, *et al.*, 2000).

There are two factors utilized in this analysis. First, the range R , this is the difference between the minimum and maximum 'accumulated' values or cumulative sum of $X(t, \tau)$ of the natural phenomenon at discrete integer-valued time t over a time span τ . Second, the standard deviation S , estimated from the observed values $X_i(t)$. Hurst found that the ratio R/S is described for a large number of natural phenomena by the following empirical relation:

$$R/S = (c \cdot \tau)^H \quad (1)$$

where τ is the time span and H is the Hurst exponent. Hurst set the coefficient c equal to 0.5. R and S are defined as:

$$R(\tau) = \max_{1 \leq t \leq \tau} X(t, \tau) - \min_{1 \leq t \leq \tau} X(t, \tau) \quad (2)$$

$$S = \left(\frac{1}{\tau} \sum_{t=1}^{\tau} \{ \xi(t) - \langle \xi \rangle_{\tau} \}^2 \right)^{1/2} \quad (3)$$

$$\langle \xi \rangle_{\tau} = \frac{1}{\tau} \sum_{t=1}^{\tau} \xi(t) \quad (4)$$

$$X(t, \tau) = \sum_{u=1}^t \{ \xi(u) - \langle \xi \rangle_{\tau} \} \quad (5)$$

The relationship between the Hurst exponent and the fractal dimension is simply $D=2-H$.

Table 4 The values of log(R/S), fractional dimension and Hurst parameter for three different solutions

Stainless steel	Solution A	Solution B	Solution C

log(R/S)	2.4114	2.3936	2.4502
D	1.0919	1.1532	1.1660
H	0.9081	0.8468	0.8340

In Table 4, the Hurst parameters of the ECN data are between 0.5 and 1, from which we can tell that the ECN signals of corrosion process of stainless steel has self-similar properties.

4. TIME-FREQUENCY ANALYSIS OF ECN SIGNALS

4.1 Time domain

Mean is the average value of potential measurements. According to Eq. [6]

$$\bar{E} = \frac{1}{N} \sum_{k=1}^N E[k] \quad (6)$$

where $E[k]$ is the potential value.

Variance is a measurement of the average AC Power in the signal. It is also referred to as noise power.

$$S = \frac{1}{N} \sum_{k=1}^N (E_n[k])^2 \quad (7)$$

Skewness is a non-dimensional measurement of the symmetry of a distribution. A zero value means that the distribution is symmetrical about the mean. A positive value indicates there is a tail in the positive direction and a negative value implies the presence of tail in the negative direction. A time record consisting of unidirectional transient will typically be heavily skewed, and this may be useful to detect transient associated with metastable pitting.

$$\text{skewness} = \frac{1}{n} \sum_{k=1}^N \left(\frac{E_n[k] - \bar{E}}{\sqrt{E_n[k]^2}} \right)^3 \quad (8)$$

Kurtosis is a measurement of whether the data are peaked or flat relative to a normal distribution. That is, data sets with high kurtosis tend to have a distinct peak near the mean, decline rapidly, and have heavy tails. Data sets with low kurtosis tend to have a flat top near the mean rather than a sharp peak. Positive kurtosis indicates a "peaked" distribution and negative kurtosis indicates a "flat" distribution.

$$\text{kurtosis} = \frac{1}{n} \sum_{k=1}^N \left(\frac{E_n[k] - \bar{E}}{\sqrt{E_n[k]^2}} \right)^4 \quad (9)$$

Noise resistance: According to Cottis and Turgoose (1999) his parameter may ultimately be used to yield a corrosion rate measurement. This is true of the LPR, EN, and EIS techniques. These resistances are related to corrosion rate by the Stern-Geary linear approximation to the Butler-Volmer equation,

$$R_p = R_n = \frac{\Delta E}{\Delta i_{\text{applied}}} = \frac{\beta_a \beta_c}{2.303(i_{\text{corr}})(\beta_a + \beta_c)} = \frac{B}{(i_{\text{corr}})} \quad (10)$$

where R_p is a polarization resistance obtained from the LPR and EIS techniques, R_n is a reaction resistance obtained from the EN technique, ΔE is the incremental change in potential measured due to the incremental change in applied current density ($\Delta i_{applied}$), B is the Stern-Geary constant, β_a and β_c are the anodic and cathodic Tafel constants, respectively, and i_{corr} is the corrosion current density from which a corrosion rate may be calculated using Faraday's Law. The Stern-Geary constant (determined by the Tafel constants) is the only variable that is normally not measured, but commonly assumed to have a value of 0.020 to 0.030 V/decade. The electrochemical noise resistance can be obtained by (11),

$$R_n = \frac{\sigma V}{\sigma I} \quad (11)$$

where $\sigma V, \sigma I$ are the standard deviations of potential and current in a given time record, respectively.

Table 5 Four order statistical components: Mean, Variance, Skewness, Kurtosis and the noise resistance of three different solutions

Stainless Steel	Solution A	Solution B	Solution C
Mean	-0.2388	-0.3192	-0.3808
Variance	1.3896e-004	2.2726e-005	4.1023e-006
Skewness	-1.4296	1.8382	0.4142
Kurtosis	3.9443	4.7590	2.5538
Noise resistance	22.5420	20.4687	26.3401

The mean value of the potential noise in Table 5 indicates that the potential noise grew from solution A to C. The Variance values indicate that the noise power is decreased from solution A to C, which means the corrosion rate is decreased. The skewness shows that solution A has a negative tail while solution B and C have positive tails. The kurtosis values show that all the potential noises are "peaked" distributions meaning they have large fluctuations. The noise resistance derived by the conventional method shows that solution B has the smallest noise resistance which indicates the highest corrosion rate. The conclusions from the noise resistance and variance values are contradictory; therefore, we cannot tell the corrosion rate from the conventional methods.

4.2 Frequency domain

Fractional Fourier transform has complexity proportional to the fast Fourier transform algorithm. In the self-similar random process applications, it is possible to improve performance by the use of the

fractional Fourier transform instead of the ordinary Fourier transform. Since the fractional transform can be computed in about the same time as the ordinary transform, these performance improvements come without additional cost. In some cases filtering in a fractional Fourier domain, rather than the ordinary Fourier domain, allows one to decrease the mean square error in estimating a distorted and noisy signal.

Fractional Fourier transform is used to find out the Power spectrum density of the potential noise. The a^{th} -order fractional Fourier transform $\{F^a f\}(x)$ of the function $f(x)$ can be defined for $0 < |a| < 2$ as

$$F^a [f(x)] \equiv \{F^a f\}(x) \equiv \int_{-\infty}^{\infty} B_a(x, x') f(x') dx' \quad (12)$$

$$B_a(x, x') \equiv A_\phi \exp[i\pi(x^2 \cot\phi - 2xx' \csc\phi + x'^2 \cot\phi)] \quad (13)$$

$$A_\phi \equiv \frac{\exp(-i\pi \operatorname{sgn}(\sin\phi)/4 + i\phi/2)}{|\sin\phi|^{1/2}} \quad (14)$$

where

$$\phi = \frac{a\pi}{2} \quad (15)$$

and i is the imaginary unit. The kernel approaches

$$B_0(x, x') \equiv \sigma(x - x')$$

$B_{\pm 2}(x, x') \equiv \sigma(x + x')$. This definition is easily extended outside the interval $[-2, 2]$ by remembering that F^{4j} is the identity operator for any integer j and that the fractional Fourier transform operator is additive in index, that is, $F^{a_1} F^{a_2} = F^{a_1 + a_2}$. A complete set of Eigen functions of the fractional Fourier transform are the Hermite-Gaussian functions:

$$F^a [\psi_n(x)] = e^{-ian\pi/2} \psi_n(x) \quad (16)$$

$$\psi_n(x) = \frac{2^{1/4}}{\sqrt{2^n n!}} H_n(\sqrt{2\pi}x) \exp(-\pi x^2) \quad (17)$$

where $H_n(x)$ is the n^{th} -order Hermite polynomial. The spectral expansion of the linear transform kernel is:

$$B_a(x, x') = \sum_{n=0}^{\infty} e^{-ian\pi/2} \psi_n(x) \psi_n(x') \quad (18)$$

Second and higher dimensional transforms have separable kernels so that most results easily generalize to higher dimensions (Ozaktas and Mendlovic, 1993, 1994; Lohmann, 1993).

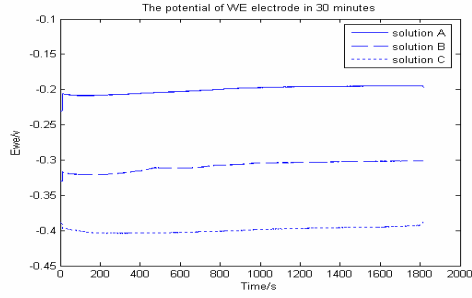


Figure 2: Potential noise of stainless steel WE electrode in three different solutions tested for 30 minutes

Figure 2 shows that there is an increase in corrosion potential of approximately 0.1 V between each solution, with solution A having the highest corrosion potential.

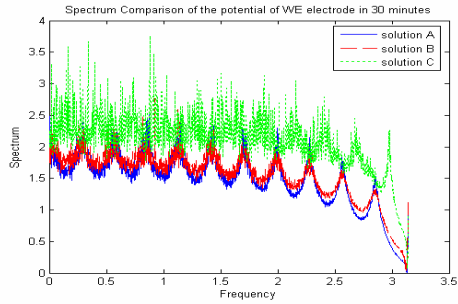


Figure 3: FFT is used to get the power spectrum of potential noise of stainless steel WE electrode in three different solutions.

The plot in Figure 3 is shown to provide a qualitative comparison between PSD of potential noise calculations for Conventional Fast Fourier Transforms and Fractional Fourier Transforms.

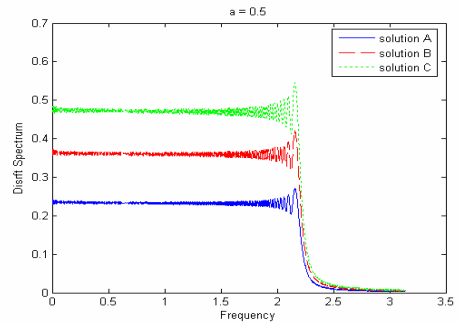


Figure 4: FrFT is used to get the power spectrum of potential noise in three different solutions when $a=0.5$.

The fast Fourier transform (FFT) of the potential noise shown in figure 2 are depicted in figure 3. The fractional Fourier transform of the potential noise shown in figure 2 are depicted in figure 4. There is an increase in the magnitude of potential noise from solution A to solution C, which is also reflected in FrFT plot. It is hard to recognize the increase between solution A and B in FFT plot, and FFT spectrum has unexpected fluctuations. In figure 4 we can clearly see that the magnitude of FFT of potential noise in solution A is larger than that of solution B, while the magnitude of FFT of potential noise in solution B is larger than that of solution C. Thus the changes in the ECN signals due to an

increase in rate of corrosion resulted in a decrease in the magnitude of the FFT.

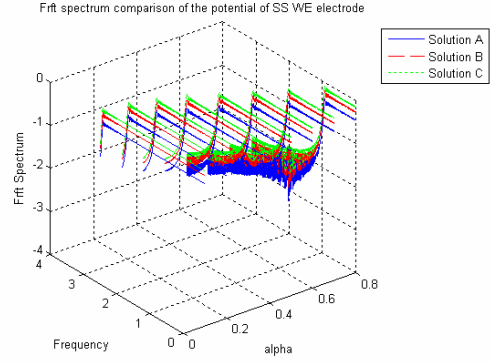


Figure 5: The power spectrum of potential noise of a stainless steel WE electrode in three different solutions using fractional Fourier transforms. The fractional order (a) varies from 0.1 to 0.8.

Figure 5 is the result of potential noise power spectrum using different ' a ' values in fractional Fourier transform. We can see that the passband is becoming shorter when ' a ' increases from 0.1 to 0.8. The plot also shows that the potential noise is dominated by low frequency components, since it is usually the low frequency information that is useful for noise impedance computations. A rough estimate of noise impedance can be obtained from the fractional Fourier transform diagrams by comparing the magnitude.

Spectral noise impedance

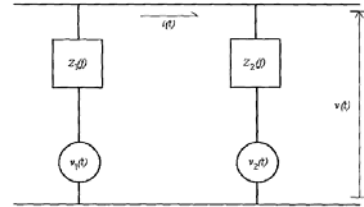


Figure 6: Equivalent circuit of a simultaneous ECN measurement

Figure 6 is described by Eden *et al.* (1986). $Z_1(f), Z_2(f)$ are the electrochemical equivalent impedances of the two electrodes, $v_1(t), v_2(t)$ are the Thevenin equivalent EN sources associated with each electrode and $v(t)$ and $i(t)$ are the measured potential noise and current noise, respectively. Bertocci *et al.* (1997) defines the spectral noise impedance as:

$$R_{sn}(f) = \sqrt{\frac{S_v(f)}{S_i(f)}} \quad (19)$$

where $S_v(f)$ is the power spectral density of the potential noise and $S_i(f)$ is the power spectral density of the current noise.

For identical impedance $Z_1(f) = Z_2(f) = Z(f)$, the spectral noise impedance can be expressed as:

$$R_{sn}(f) = |Z(f)| \quad (20)$$

Bertocci, *et al.* (1997), derived the relationship between noise resistance R_n and spectral noise impedance R_{sn} as:

$$R_n = \left[\frac{\int_{f_{\min}}^{f_{\max}} S_i(f) R_{sn}^2(f) df}{\int_{f_{\min}}^{f_{\max}} S_i(f) df} \right]^{1/2} \quad (21)$$

where f is the frequency in Hz, f_{\min} is the lower limit of the frequency (equal to two times the inverse measurement time), and f_{\max} is the higher limit frequency (equal to one half of the sampling frequency). If f_{\min} is sufficiently low, R_n can be expressed by: $R_n = R_{sn}(f \rightarrow 0)$ (22)

Here we use fractional Fourier transform for the spectral noise impedance. We can get the figure below.

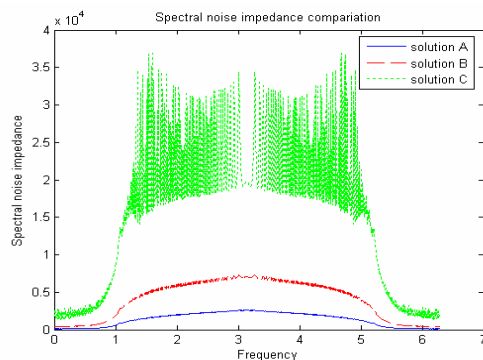


Figure 7: Spectral noise impedances of solution A, B and C derived by fractional Fourier transform

Figure 7 shows that the spectral noise impedance of solution C is the largest of the three impedances, and the spectral noise impedance of solution A is the smallest. According to Eq.[10] the corrosion rate is inversely proportional to the noise impedance. Therefore, both Figure 7 and the mathematics confirm that the corrosion rate of solution A is higher than that of solution B, and the corrosion rate of solution B is higher than that of solution C.

5. CONCLUSION

The corrosion rate of the three different simulated saliva solutions follows this order: **Sol. A > Sol. B > Sol. C**. Analysis of ECN signals in both time and frequency domains are presented. R/S analysis shows that the ECN signals have self-similar properties which cause the conventional analysis methods to perform poorly. It has been shown in this paper that Fractional Fourier transforms can successfully be used for analysis of electrochemical noise data. It is also a useful technique for analysis of self-similar signals. Impedance data obtained from the fractional Fourier transform can yield the corrosion rate. The R/S analysis and fractional Fourier transform are two examples of fractional order signal processing that can be applied to electrochemical data.

ACKNOWLEDGEMENT: This work is gratefully supported by USU College of Engineering "Skunk works" Seed Grant program.

REFERENCES

- Almeida, L. B. (1994). The fractional Fourier transform and time-frequency representations." *IEEE Trans. Sig. Proc.*, (42):3084-3091.
- Devynck, P., G. Wang, G. Antar, G. Bonhomme (2000). The Hurst exponent and long-time correlation. *27th EPS Conference on Contr. Fusion and Plasma Phys. Budapest*, 12-16 June 2000 ECA Vol. 24B, pp. 632-635.
- Duffó, G. S., and E. Quezada Castillo (2004). Development of an Artificial Saliva Solution for Studying the Corrosion Behavior of Dental Alloys. *NACE International*, Vol. 60, No6.
- Eden, D. A., K. Hladky, D.G. John, and J.L. Dawson (1986). Electrochemical noise – simultaneous Monitoring of potential and current noise signals from corroding electrodes. *Proc. of Corrosion 86*. National Association of Corrosion Engineering.
- Feder, J. (1988). *Fractals*. pp. 149-183. Plenum Press.
- Fonollosa, J. R. and C. L. Nikias (1994). A new positive time-frequency distribution. *Proc. IEEE Int. Conf. Acoust., Speech, Signal Processing*, pp. IV-301-IV-304.
- Gabrielli, C., F. Huet, M. Keddam (1985). Characterization of electrolytic bubble evolution by Spectral analysis. *J. Appl. Electrochem.* V.15, p. 503.
- Leontitsis, A. (2004). Rescaled Range Analysis. http://www.mathworks.com/Matlab_central/fileexchange/loadFile.do?objectId=4325&objectType=file
- Lohmann, A. W. (1993). Image rotation, Wigner rotation and the fractional Fourier transform. *J. Opt. Soc. Amer. A*, Vol. 10, pp. 2181-2186.
- Lowe, A. M., and H. Eren (2000). Signal analysis and synthesis as applied to electrochemical noise in corrosion, *TENCON 2000. Proc.*, Vol.1, pp. 240 – 245.
- Lowe, A. M. (2002). Corrosion signal processing using wavelet analysis and Nyquist diagrams. *Proc. of the 19th IEEE Instrum. and Measur. Tech. Conf.*, 2002. V. 1, pp. 855 – 860.
- Mandelbrot, B. B. and J.R. Wallis (1968). Noah, Joseph and operational hydrology. *Water Resources Research*, Vol. 4, pp. 909-918.
- Mendlovic, D. and H. M. Ozaktas (1993). Fractional Fourier transformations and their optical implementation: Part I. *J. Opt. Soc. Amer. A*, Vol. 10, pp. 1875-1881.
- Mendlovic, D., H. M. Ozaktas (1995), and A. W. Lohmann. Fractional correlation. *Appl. Opt.*, Vol. 34, pp. 303-309.
- Meredith, D. O., L. Eschbach, M. A. Wood, M. O. Riehle, Adam S.G. Curtis, R. G. Richards (2005). Human fibroblast reactions to standard and electropolished titanium and Ti-6Al-7Nb, and electropolished stainless steel. *J Biomed Mater Res 75A*, pp. 541-555.
- Ozaktas, H. M. and D. Mendlovic (1993). Fourier transforms of fractional order and their optical interpretation. *Opt. Commun.*, (101):163-169.
- Ozaktas, H. M. and D. Mendlovic (1993). Fractional Fourier transformations and their optical implementation: Part II. *J. Opt. Soc. Amer. A*, Vol. 10, pp. 2522-2531.
- Ozaktas, H. M., B. Barshan, D. Mendlovic, and L. Onural (1994). Convolution, filtering, and multiplexing in fractional Fourier domains and their relation to chirp and wavelet transforms. *J. Opt. Soc. Amer. A*, Vol. 11, pp. 547-559.
- Ozaktas, H. M., M. A. Kutay, and G. Bozdagi (1996). Digital computation of the fractional Fourier transform. *IEEE Trans. Sig. Proc.*, Vol. 44, pp. 2141-2150.